

Article

Hybrid Boron-Carbon Chemistry

Josep M. Oliva-Enrich ^{1,*} , Ibon Alkorta ²  and José Elguero ²¹ Instituto de Química-Física “Rocasolano” (CSIC), Serrano 119, E-28006 Madrid, Spain² Instituto de Química Médica (CSIC), Juan de la Cierva, 3, E-28006 Madrid, Spain; ibon@iqm.csic.es (I.A.); iqmbe17@iqm.csic.es (J.E.)

* Correspondence: j.m.oliva@iqfr.csic.es; Tel.: +34-91-561-9400

Academic Editor: Ashok Kakkar

Received: 18 September 2020; Accepted: 26 October 2020; Published: 29 October 2020



Abstract: The recently proved one-to-one structural equivalence between a conjugated hydrocarbon C_nH_m and the corresponding borane B_nH_{m+n} is applied here to hybrid systems, where each C=C double bond in the hydrocarbon is consecutively substituted by planar $B(H_2)B$ moieties from diborane(6). Quantum chemical computations with the B3LYP/cc-pVTZ method show that the structural equivalences are maintained along the substitutions, even for non-planar systems. We use as benchmark aromatic and antiaromatic (poly)cyclic conjugated hydrocarbons: cyclobutadiene, benzene, cyclooctatetraene, pentalene, benzocyclobutadiene, naphthalene and azulene. The transformation of these conjugated hydrocarbons to the corresponding boranes is analyzed from the viewpoint of geometry and electronic structure.

Keywords: boron; conjugated hydrocarbon; isoelectronic molecule; electronic structure; quantum chemistry; singlet-triplet gap

1. Introduction

Planar conjugated hydrocarbons played a key role in the early days of quantum mechanics, when computers were not available, and physical models were needed in order to understand the electronic structure of molecules [1], the attractive nature of the chemical bond [2], the nature of ground and excited states in atoms and molecules [3–5], and mechanistical studies of chemical reactions [6].

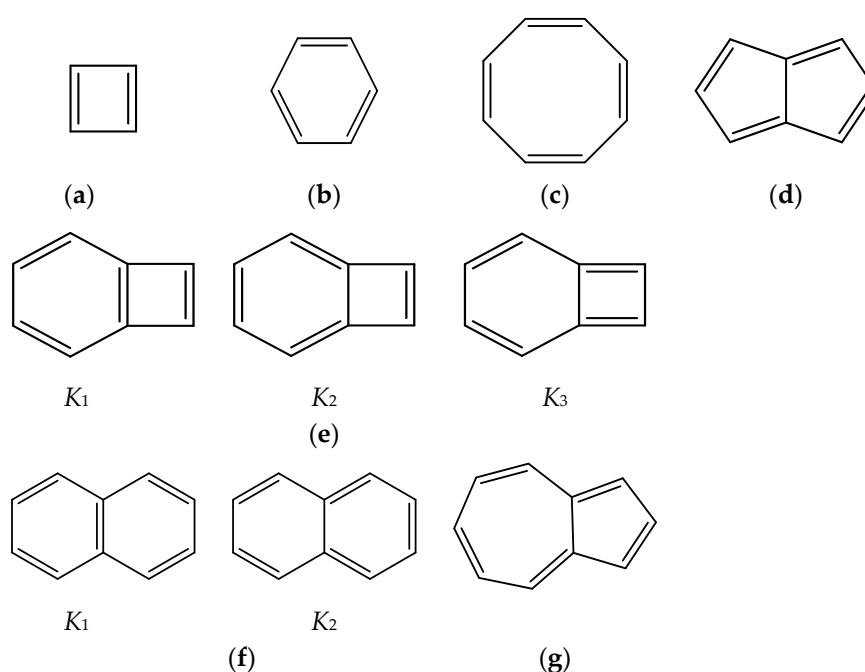
On the other hand, a relevant quantity in chemistry is the energy gap between the lowest-lying singlet and triplet electronic states in a molecule, directly related to the reactivity of the system, and useful, e.g., for the design of photochemical molecular devices [7]. For instance, methylene CH_2 is a very reactive species with a triplet ground state and a singlet-triplet experimental energy gap of $38 \text{ kJ}\cdot\text{mol}^{-1}$ [8]. On the other hand, water H_2O has a singlet ground state with an experimental singlet-triplet energy gap of $675 \text{ kJ}\cdot\text{mol}^{-1}$ [9]. Hence, the larger the singlet-triplet energy gap the more stable a molecule.

The chemistry of boron compounds has evolved along the second half of the XXth century and beginning of the XXIst century in a generalised dual fashion since the original works of Stock [10] on B_nH_m boranes syntheses in the beginning of the XXth century: (i) organoboron [11] and metal-boron [12] chemistry and (ii) the chemistry of 3D polyhedral (metalla)heteroborane structures [13–17]. Given the huge and magnificent efforts done towards the synthesis of new boron derivatives in the last decades, a complete literature citation here is impractical.

The recent experimental isolation of borophane layers [18], a 2D $(BH)_1$ system structurally equivalent to graphene and the characterisation of chemical structures where one C=C double bond is substituted by one $B(H_2)B$ moiety [19–23] calls for the possibility of creating a new field of research within boron chemistry, namely, the synthesis of finite planar neutral borane molecules. We have recently proved that there is a one-to-one structural correspondence between any planar conjugated

hydrocarbon C_nH_m and the planar borane $B_nH_{(m+n)}$, indeed with the same number of electrons and n more hydrogen atoms in the latter [24]. This transformation can be carried out by substituting all C=C double bonds by a perpendicular planar $B(H_2)B$ moiety, which is the central rhombus of diborane(6). Up to this date we have not found any exception so far to this transformation and is extended here to non-planar systems.

The problems that we would like to tackle in this work, dedicated to Professor Todd B. Marder on the occasion of his 65th birthday, are related to the stability of hybrid boron-carbon isoelectronic chemical structures built by consecutive substitution of C=C by $B(H_2)B$ moieties in (poly)cyclic conjugated hydrocarbons. Particularly, we have chosen examples with $4n$ π electrons: cyclobutadiene, cyclooctatetraene, pentalene and benzocyclobutadiene, and examples with $(4n + 2)$ π electrons: benzene, naphthalene and azulene. The question we would like to answer here is: Given a (poly)cyclic conjugated hydrocarbon C_nH_m with an even number of carbon atoms or π electrons, how similar or different are the hybrid systems $C_{(n-2k)}B_{(2k)}H_{(m+2k)}$, with $k = \{0, 1, 2, \dots, n/2\}$, to the original hydrocarbon from the structural and electronic structure point of view? In Scheme 1 we gather the conjugated hydrocarbons considered in this work.



Scheme 1. Conjugated hydrocarbons included in this work. Kekulé structures K_i [25] are also included for those structures leading to different hybrid isomers on $\{C=C \leftrightarrow B(H_2)B\}$ substitutions. (a) cyclobutadiene, (b) benzene, (c) cyclooctatetraene, (d) pentalene, (e) benzocyclobutadiene with Kekulé structures K_1 , K_2 and K_3 , (f) naphthalene with Kekulé structures K_1 and K_2 , and (g) azulene. All systems are planar, except for cyclooctatetraene (c) with a D_{2d} symmetry energy minimum.

2. Results

Tables 1–5 gather the formula, structure, electronic energy, vertical singlet-triplet energy gaps and point-group symmetry (PGS) for all the systems included in this work, derived from a conjugated hydrocarbon C_nH_m with an even number of carbon atoms or π electrons and the structures derived from consecutive $k \{ C=C \leftrightarrow B(H_2)B \}$ substitutions, with $1 \leq k \leq n/2$. The triplet energy is computed with optimized geometry of the singlet ground state due to considerable geometrical changes in triplet optimizations, and therefore singlet-triplet energies are vertical. From cyclooctatetraene onwards, all $C_{(n-2k)}B_{(2k)}H_{(m+2k)}$ structures have more than one isomer, for $1 \leq k < n/2$. Hence, one might inquire the extent of change in energy differences and singlet-triplet energies in different isomers of a given structure. When isomers arise under $k \{ C=C \leftrightarrow B(H_2)B \}$ substitutions in a given

structure, these are labelled as {(I), (II), ... } and ordered in increasing energy, as displayed in Figures 1–5. All structures and isomers correspond to planar structures, except for cyclooctatetraene C_8H_8 ($k = 0$) and structures $C_{(8-2k)}B_{(2k)}H_{(8+2k)}$ ($k = 1-4$). All structures and isomers presented in this work, as computed with the B3LYP/cc-pVTZ model, correspond to energy minima. B3LYP/cc-pVTZ optimised geometries, in cartesian coordinates (Å), of the systems included in the work are presented in Supplementary Materials.

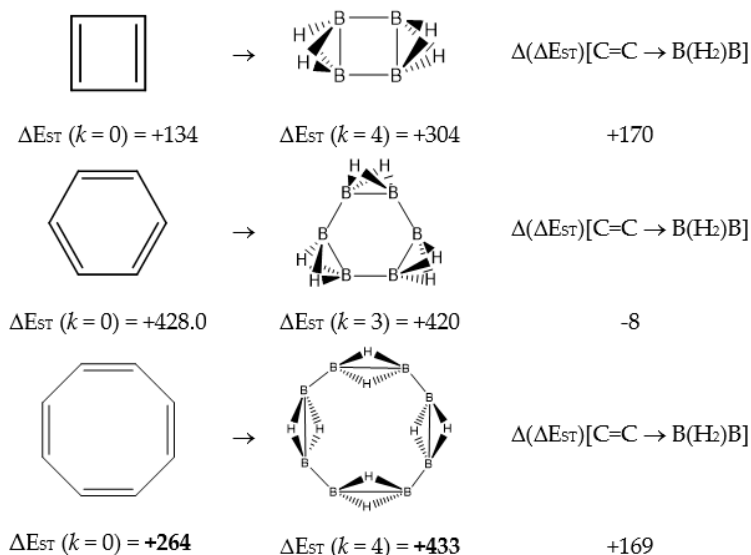


Figure 1. Singlet-triplet gap ΔE_{ST} (kJ·mol⁻¹) for cyclobutadiene, benzene and cyclooctatetraene and the equivalent B_nH_{m+n} structures, and the differences $\Delta(\Delta E_{ST})[C=C \rightarrow B(H_2)B] = \Delta E_{ST}(B_nH_{m+n}) - \Delta E_{ST}(C_nH_m)$.

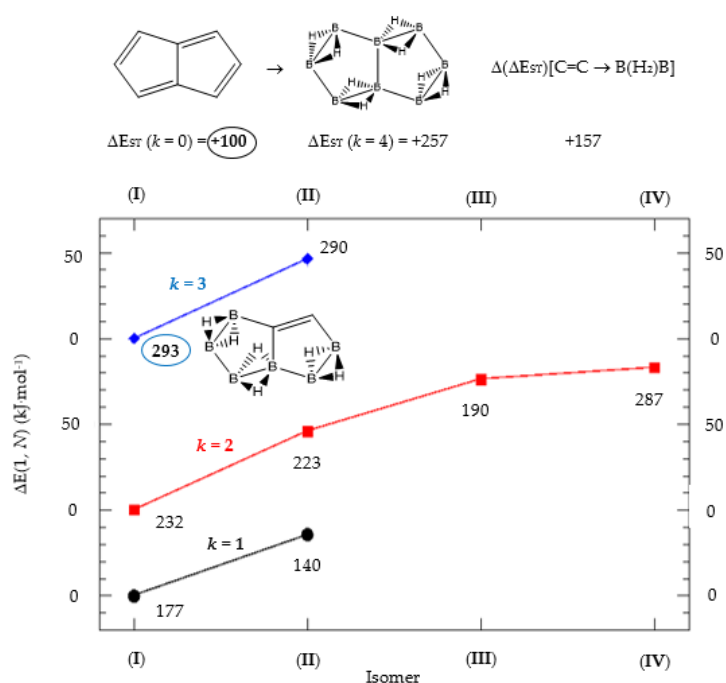


Figure 2. Isomer structure vs. $\Delta E(I, N_{iso})$ (kJ·mol⁻¹) for pentalene, with $\Delta E(I, N) = E(N_{iso}) - E(I)$. N_{iso} is the number of isomers for a given k in $C_{(n-2k)}B_{(2k)}H_{(m+2k)}$. In addition, for each structure the singlet-triplet gap is shown (kJ·mol⁻¹). The encircled singlet-triplet energy gaps correspond to the maximum and minimum values.

Table 1. Cyclobutadiene, benzene, cyclooctatetraene and the corresponding hybrids $C_{(n-2k)}B_{(2k)}H_{(m+2k)}$, with formula (k), structure, energies (B3LYP/*cc*-pVTZ, in au), singlet-triplet vertical energy gaps ($\text{kJ}\cdot\text{mol}^{-1}$) with the B3LYP and B97D functionals, $\Delta E_{\text{ST,B3LYP}}$ and $\Delta E_{\text{ST,B97D}}$ (italic) respectively, and point-group symmetry (PGS) in parentheses. For benzene and hybrids we also show the molecular electrostatic potential (MEP) on the 0.001 au electron density isosurface (blue and red colors indicate values $V(r) > +0.015$ au and $V(r) < -0.015$ au, respectively), and the anisotropy of the induced current density (ACID). Different isomers of a given structure are labelled as {**(I)**, **(II)**, ... } and ordered in increasing energy. All geometries correspond to energy minima. In-plane *exo* hydrogen atoms bound to carbon and boron not shown for clarity. B3LYP/*cc*-pVTZ computations.

Cyclobutadiene $C_{(4-2k)}B_{(2k)}H_{(4+2k)}$					
Formula (k)	C_4H_4 (0)	$C_2B_2H_6$ (1)	B_4H_8 (2)		
Structure					
Energy	-154.734983	-129.488436	-104.182558		
$\Delta E_{\text{ST,B3LYP}}$ (PGS)	133.5 (D_{2h})	272.9 (C_{2v})	303.6 (D_{2h})		
$\Delta E_{\text{ST,B97D}}$	124.8	265.2	272.3		
Benzene $C_{(6-2k)}B_{(2k)}H_{(6+2k)}$					
Formula (k)	C_6H_6 (0)	$C_4B_2H_8$ (1)	$C_2B_4H_{10}$ (2)	B_6H_{12} (3)	
Structure					
MEP					
ACID					
Energy	-232.333368	-206.929239	-181.596841	-156.324833	
$\Delta E_{\text{ST,B3LYP}}$ (PGS)	428.0 (D_{6h})	325.9 (C_{2v})	361.2 (C_{2v})	419.8 (D_{3h})	
$\Delta E_{\text{ST,B97D}}$	414.4	312.9	353.1	373.2	
Cyclooctatetraene $C_{(8-2k)}B_{(2k)}H_{(8+2k)}$					
Formula (k)	C_8H_8 (0)	$C_6B_2H_{10}$ (1)	$C_4B_4H_{12}$ (2)	$C_2B_6H_{14}$ (3)	B_8H_{16} (4)
Structure					
Energy	-309.697808	-284.398420	-259.096253	-233.769903	-208.442935
$\Delta E_{\text{ST,B3LYP}}$ (PGS)	264.4 (D_{2d})	312.2 (C_s)	(I) 377.1 (C_{2v})	375.3 (C_s)	433.1 (D_{2d})
$\Delta E_{\text{ST,B97D}}$	234.3	284.1	344.2	364.4	381.0
Energy			-259.084995		
$\Delta E_{\text{ST,B3LYP}}$ (PGS)			(II) 355.7 (C_2)		
$\Delta E_{\text{ST,B97D}}$			332.9		

Table 2. Pentalene and the corresponding hybrids $C_{(8-2k)}B_{(2k)}H_{(6+2k)}$, with formula (k), structure, energies (au), singlet-triplet vertical energy gaps ΔE_{ST} ($\text{kJ}\cdot\text{mol}^{-1}$) and point-group symmetry (PGS) in parentheses. Different isomers of a given structure are labelled as {(I), (II), ... } and ordered in increasing energy. All geometries correspond to energy minima. In-plane *exo* hydrogen atoms bound to carbon and boron not shown for clarity. B3LYP/cc-pVTZ computations.

Pentalene $C_{(8-2k)}B_{(2k)}H_{(6+2k)}$				
C_8H_6 (0)	$C_6B_2H_8$ (1)	$C_4B_4H_{10}$ (2)	$C_2B_6H_{12}$ (3)	B_8H_{14} (4)
-308.476075 100.1 (C_{2h})	-283.193095 (I) 176.7 (C_s)	-257.898516 (I) 232.3 (C_{2h})	-232.562207 (I) 292.9 (C_s)	-207.215121 257.3 (C_{2h})
	-283.179450 (II) 140.2 (C_s)	-257.881067 (II) 222.5 (C_s)	-232.544645 (II) 290.4 (C_s)	
		-257.869529 (III) 189.9 (C_s)		
		-257.866865 (IV) 286.8 (C_{2h})		

Table 3. a. Benzocyclobutadiene Kekulé structures K_1 and the corresponding hybrid boranes, with formula (k), structure, energies (au), singlet-triplet vertical energy gaps ΔE_{ST} ($\text{kJ}\cdot\text{mol}^{-1}$) and point-group symmetry (PGS) in parentheses. **b.** Kekulé structures K_2 . **c.** Kekulé structures K_3 . Different isomers of a given structure are labelled as {(I), (II), ... } and ordered in increasing energy. B3LYP/cc-pVTZ computations. All geometries correspond to energy minima. In-plane *exo* hydrogen atoms bound to carbon and boron not shown for clarity.

(a)				
Benzocyclobutadiene Kekulé Structure K_1 : $C_{(8-2k)}B_{(2k)}H_{(6+2k)}$				
C_8H_6 (0)	$C_6B_2H_8$ (1)	$C_4B_4H_{10}$ (2)	$C_2B_6H_{12}$ (3)	B_8H_{14} (4)
-308.466884 195.3 (C_{2v})	-283.206069 (I) 303.0 (C_{2v})	-257.868229 (I) 225.8 (C_s)	-232.534049 (I) 361.7 (C_{2v})	-207.187765 264.0 (C_{2v})

Table 3. Cont.

(a)				
Benzocyclobutadiene Kekulé Structure K_1 : $C_{(8-2k)}B_{(2k)}H_{(6+2k)}$				
C_8H_6 (0)	$C_6B_2H_8$ (1)	$C_4B_4H_{10}$ (2)	$C_2B_6H_{12}$ (3)	B_8H_{14} (4)
	-283.141948 (II) 285.1 (C_{2v})	-257.847770 (II) 338.7 (C_{2v})	-232.521784 (II) 308.5 (C_s)	
	-283.125618 (III) 117.7 (C_s)	-257.820144 (III) 265.9 (C_s)	-232.488989 (III) 254.3 (C_{2v})	
		-257.791707 (IV) 108.4 (C_{2v})		
(b)				
Benzocyclobutadiene Kekulé Structure K_2 : $C_{(8-2k)}B_{(2k)}H_{(6+2k)}$				
C_6H_6 (0)	$C_6B_2H_8$ (1)	$C_4B_4H_{10}$ (2)	$C_2B_6H_{12}$ (3)	B_6H_{14} (4)
-308.466884 195.3 (C_{2v})	-283.206069 (I) C_{2v} 302.9 = (I) in K_1	-257.880840 (I) C_{2v} 367.5	-232.542344 (I) C_s 342.3	-207.194531 C_{2v} 310.3
	-283.162243 (II) C_{2v} 267.2	-257.869238 (II) C_s 280.1	-232.529224 (II) C_{2v} 323.8	
	-283.161645 (III) C_s 220.2	-257.848002 (III) C_s 280.4	-232.517824 (III) C_{2v} 348.8	
		-257.842989 (IV) C_{2v} 328.5		

Table 3. Cont.

(c)				
Benzocyclobutadiene Kekulé Structure K_3 : $C_{(8-2k)}B_{(2k)}H_{(6+2k)}$				
C_8H_6 (0)	$C_6B_2H_8$ (1)	$C_4B_4H_{10}$ (2)	$C_2B_6H_{12}$ (3)	B_6H_{14} (4)
-308.466884 195.3 (C_{2v})	-283.151132 (I) 137.7 (C_s)	-257.848644 (I) 229.1 (C_s)	-232.527701 (I) 210.9 (C_s)	-207.196234 374.0 (C_{2v})
	-283.125618 (II) 117.6 (C_s)	-257.841430 (II) 219.6 (C_{2v})	-232.517894 (II) 237.0 (C_s)	
		-257.838383 (III) 173.8 (C_s)		
		-257.791707 (IV) 108.5 (C_{2v})		

Table 4. a. Naphthalene Kekulé structures K_1 and the corresponding hybrid boranes, with formula (k), structure, energies (au), singlet-triplet vertical energy gaps ΔE_{ST} ($\text{kJ}\cdot\text{mol}^{-1}$) and point-group symmetry (PGS) in parentheses. **b.** Kekulé structures K_2 . Different isomers of a given structure are labelled as {(I), (II), ...} and ordered in increasing energy. B3LYP/cc-pVTZ computations. All geometries correspond to energy minima. In-plane *exo* hydrogen atoms bound to carbon and boron not shown for clarity.

(a)					
Naphthalene Kekulé Structure K_1 : $C_{(10-2k)}B_{(2k)}H_{(8+2k)}$					
$C_{10}H_8$ (0)	$C_8B_2H_{10}$ (1)	$C_6B_4H_{12}$ (2)	$C_4B_6H_{14}$ (3)	$C_2B_8H_{16}$ (4)	$B_{10}H_{18}$ (5)
-386.025545 304.3 (D_{2h})	-360.701217 (I) 325.9 (C_s)	-335.372607 (I) 414.4 (C_{2v})	-310.030119 (I) 287.8 (C_s)	-284.691550 (I) 316.1 (D_{2h})	-259.335521 313.6 (D_{2h})

Table 4. Cont.

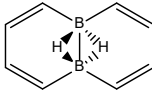
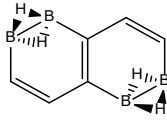
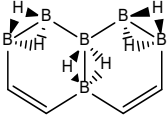
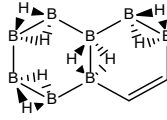
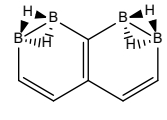
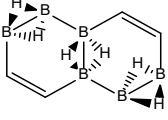
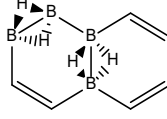
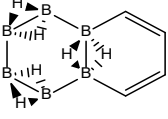
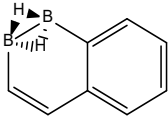
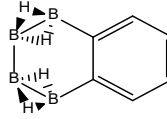
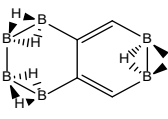
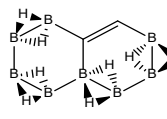
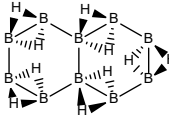
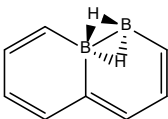
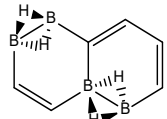
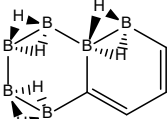
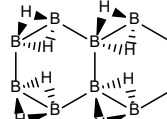
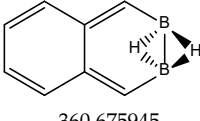
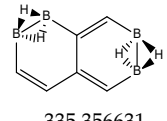
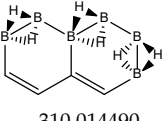
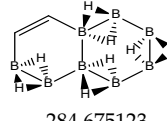
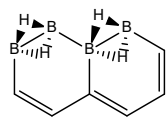
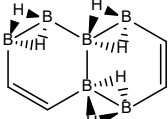
(a)					
Naphthalene Kekulé Structure $K_1: C_{(10-2k)}B_{(2k)}H_{(8+2k)}$					
$C_{10}H_8$ (0)	$C_8B_2H_{10}$ (1)	$C_6B_4H_{12}$ (2)	$C_4B_6H_{14}$ (3)	$C_2B_8H_{16}$ (4)	$B_{10}H_{18}$ (5)
					
	−360.673209 (II) 340.7 (D_{2h})	−335.365370 (II) 266.4 (C_{2h})	−310.015638 (II) 393.0 (C_{2v})	−284.676167 (II) 353.7 (C_s)	
					
		−335.364766 (III) 300.4 (C_{2v})	−310.013813 (III) 385.0 (C_{2h})		
					
		−335.346472 (IV) 322.7 (C_s)	−310.011145 (IV) 327.6 (C_{2v})		
(b)					
Naphthalene Kekulé Structure $K_2: C_{(10-2k)}B_{(2k)}H_{(8+2k)}$					
$C_8B_2H_{10}$ (1)	$C_6B_4H_{12}$ (2)	$C_4B_6H_{14}$ (3)	$C_2B_8H_{16}$ (4)	$B_{10}H_{18}$ (5)	
					
−360.701217 (I) 325.9 (C_s) = (I) in K_1	−335.372607 (I) 414.4 (C_{2v}) = (I) in K_1	−310.028387 (I) 297.5 (C_{2v})	−284.687476 (I) 331.2 (C_s)	−259.338265 307.0 (C_{2v})	
					
−360.678565 (II) 223.1 (C_s)	−335.362684 (II) C_s 303.3	−310.025977 (II) 301.6 (C_s)	−284.679641 (II) C_{2v} 351.0		
					
−360.675945 (III) C_{2v} 187.8	−335.356631 (III) 256.1 (C_s)	−310.014490 (III) C_s 251.0	−284.675123 (III) 313.2 (C_s)		
					
	−335.352046 (IV) 244.0 (C_s)	−310.014211 (IV) 333.7 (C_s)			

Table 4. Cont.

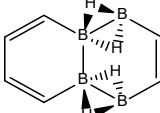
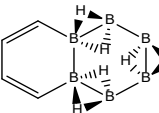
(b)				
Naphthalene Kekulé Structure K_2 : $C_{(10-2k)}B_{(2k)}H_{(8+2k)}$				
$C_8B_2H_{10}$ (1)	$C_6B_4H_{12}$ (2)	$C_4B_6H_{14}$ (3)	$C_2B_8H_{16}$ (4)	$B_{10}H_{18}$ (5)
				
	-335.335292 (V) C_{2v} 252.3	-309.998099 (V) C_{2v} 234.9		

Table 5. Azulene the corresponding hybrid boranes, with formula (k), structure, energies (au), singlet-triplet vertical energy gaps ΔE_{ST} ($\text{kJ}\cdot\text{mol}^{-1}$) and point-group symmetry (PGS) in parentheses. Different isomers of a given structure are labelled as {(I), (II), ... } and ordered in increasing energy. B3LYP/cc-pVTZ computations. All geometries correspond to energy minima. In-plane *exo* hydrogen atoms bound to carbon and boron not shown for clarity. All structures and isomers have C_s symmetry except azulene $C_{10}H_8$ and the equivalent boron structure $B_{10}H_{18}$ both with C_{2v} symmetry.

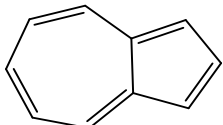
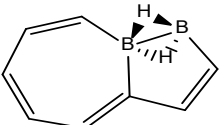
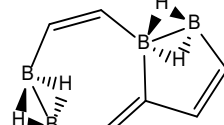
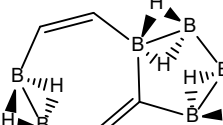
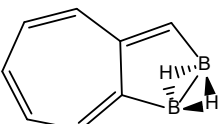
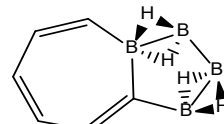
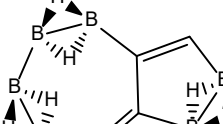
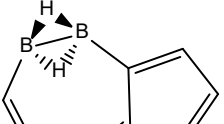
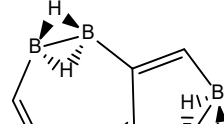
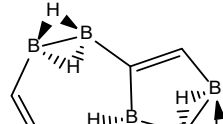
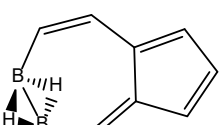
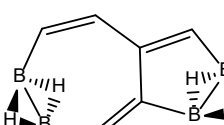
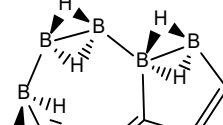
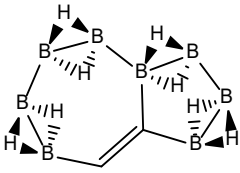
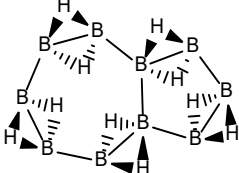
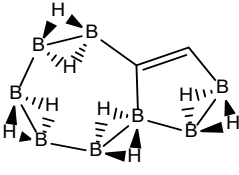
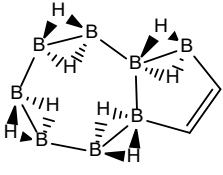
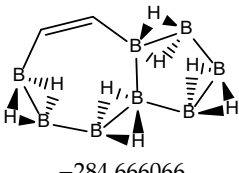
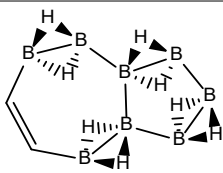
Azulene $C_{(10-2k)}B_{(2k)}H_{(8+2k)}$			
$C_{10}H_8$ (0)	$C_8B_2H_{10}$ (1)	$C_6B_4H_{12}$ (2)	$C_4B_6H_{14}$ (3)
			
-385.971486 196.3 (C_{2v})	-360.664485 (I) 224.4 (C_s)	-335.342898 (I) 260.7 (C_s)	-310.017400 (I) 329.9 (C_s)
			
	-360.653691 (II) 180.5 (C_s)	-335.338375 (II) 235.9 (C_s)	-310.010310 (II) 252.5 (C_s)
			
	-360.644455 (III) 203.1 (C_s)	-335.335924 (III) 207.6 (C_s)	-310.009032 (III) 335.1 (C_s)
			
	-360.643019 (IV) 183.3 (C_s)	-335.333474 (IV) 239.7 (C_s)	-310.006879 (IV) 248.1 (C_s)

Table 5. Cont.

Azulene $C_{(10-2k)}B_{(2k)}H_{(8+2k)}$			
$C_{10}H_8$ (0)	$C_8B_2H_{10}$ (1)	$C_6B_4H_{12}$ (2)	$C_4B_6H_{14}$ (3)
	-360.637439 (V) 179.7 (C_s)	-335.332218 (V) 212.6 (C_s)	-310.005650 (V) 250.4 (C_s)
Azulene $C_{(10-2k)}B_{(2k)}H_{(8+2k)}$			
$C_6B_4H_{12}$ (2)		$C_4B_6H_{14}$ (3)	
-335.324248 (VI) 219.3 (C_s)		-309.999674 (VI) 327.6 (C_s)	
-335.321141 (VII) 272.0 (C_s)		-309.999405 (VII) 319.5 (C_s)	
-335.320601 (VIII) 217.0 (C_s)		-309.996626 (VIII) 249.8 (C_s)	
-335.319266 (IX) 208.9 (C_s)		-309.992937 (IX) 210.9 (C_s)	
-335.313370 (X) 163.1 (C_s)		-309.989768 (X) 262.6 (C_s)	

Table 5. Cont.

Azulene $C_{(10-2k)}B_{(2k)}H_{(8+2k)}$	
$C_2B_8H_{16}$ (4)	$B_{10}H_{18}$ (5)
 <p>-284.679284 (I) 315.4 (C_s)</p>	 <p>-259.332171 (I) 293.3 (C_s)</p>
 <p>-284.675773 (II) 311.6 (C_s)</p>	
 <p>-284.667945 (III) 320.1 (C_s)</p>	
 <p>-284.666066 (IV) 317.1 (C_s)</p>	
 <p>-284.666006 (V) 313.2 (C_s)</p>	

At this point we should emphasize the geometrical changes that a C_nH_m conjugated hydrocarbon undergoes through k $\{C=C \leftrightarrow B(H_2)B\}$ substitutions, with $k = \{0, 1, 2, \dots, n/2\}$, in a given hybrid boron-carbon $C_{(n-2k)}B_{(2k)}H_{(m+2k)}$ structure.

In Table 1 and Figure 1, we gather the structures, energies and singlet-triplet gaps for cyclobutadiene, benzene and cyclooctatetraene and the corresponding $C_{(n-2k)}B_{(2k)}H_{(m+2k)}$ structures. We start off with the series for $n = 4$ in cyclobutadiene: $C_{(4-2k)}B_{(2k)}H_{(4+2k)}$, with $k = \{0, 1, 2\}$. Given the antiaromatic nature of cyclobutadiene, this molecule is very reactive with tendency to dimerize and can be observed by matrix isolation below 35 K [26]. Substitution of one $\{C=C\}$ moiety by one $\{B(H_2)B\}$ moiety in C_4H_4 ($k = 1$) leads to a $C_2B_2H_6$ cyclic structure, with a singlet-triplet energy gap $140 \text{ kJ}\cdot\text{mol}^{-1}$ larger than in C_4H_4 . A second $\{C=C \leftrightarrow B(H_2)B\}$ substitution in C_4H_4 ($k = 2$) leads to cyclic tetraborane(8), with a even larger singlet-triplet energy gap, $170 \text{ kJ}\cdot\text{mol}^{-1}$ higher than in C_4H_4 .

The next system to be analyzed is aromatic benzene ($n = 6$) and the boron-carbon hybrids: $C_{(6-2k)}B_{(2k)}H_{(6+2k)}$, with $k = \{0, 1, 2, 3\}$, as gathered in Table 1 and Figure 1. Benzene is a colorless liquid, with a characteristic odor, volatile, very flammable and carcinogenic. This molecule is the paradigm of Hückel theory [1] and the concept of aromaticity itself, with a very interesting debate reaching our days on the role of its correlation energy and the π electron spin-pairing [27]. As opposed to the previous example, the singlet-triplet energy gaps for benzene and cyclic hexaborane(12) B_6H_{12} are quite similar, $8 \text{ kJ}\cdot\text{mol}^{-1}$ larger in benzene, due to the aromatic nature of the latter. The first $\{C=C \leftrightarrow B(H_2)B\}$ substitution in benzene leading to $C_4B_2H_8$ ($k = 1$) decreases the singlet-triplet energy gap by more than $100 \text{ kJ}\cdot\text{mol}^{-1}$ —due to aromaticity loss—but with further $\{C=C \leftrightarrow B(H_2)B\}$ substitutions the singlet-triplet energy gaps increase by $35 \text{ kJ}\cdot\text{mol}^{-1}$ and $60 \text{ kJ}\cdot\text{mol}^{-1}$ for $C_2B_4H_{10}$ ($k = 2$) and B_6H_{12} ($k = 3$) respectively. This is a clear indication that breaking the aromaticity of benzene leads, to a first instance, to a less stable structure. However, this stability is increased by along the series for $k = \{2, 3\}$, and three $\{C=C \leftrightarrow B(H_2)B\}$ substitutions leads to a structure— D_{3h} cyclic hexaborane(12) B_6H_{12} —with a singlet-triplet energy gap which is only $8 \text{ kJ}\cdot\text{mol}^{-1}$ lower as compared to benzene. This result is striking and remains at the very origin of the recent proposal we have put forward [24]: To every (poly)cyclic planar conjugated hydrocarbon C_nH_m there corresponds a boron equivalent structure B_nH_{m+n} which is also an energy minimum.

Inclusion of empirical dispersion corrections with the B97D functional [28] shows a systematic decrease of the singlet-triplet energy gaps as compared to the B3LYP results, following a similar tendency, except for the complete borane structures B_nH_{m+n} with considerably lowering of $47 \text{ kJ}\cdot\text{mol}^{-1}$ for cyclic hexaborane(12), as compared to the B3LYP results. For the cyclooctatetraene series the lowering is also noteworthy when including dispersion corrections in the functional; the structure of the stationary points—energy minima—is maintained with both functionals. As described below in the Discussion section, the bond distances are slightly elongated when dispersion corrections are included, which is in agreement with lower singlet-triplet energy gaps.

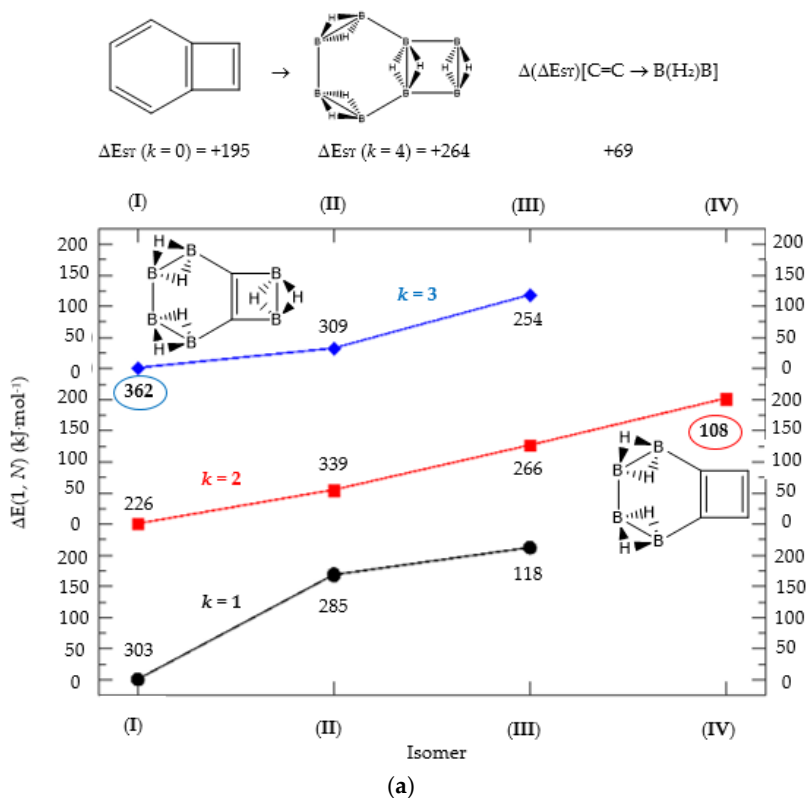


Figure 3. Cont.

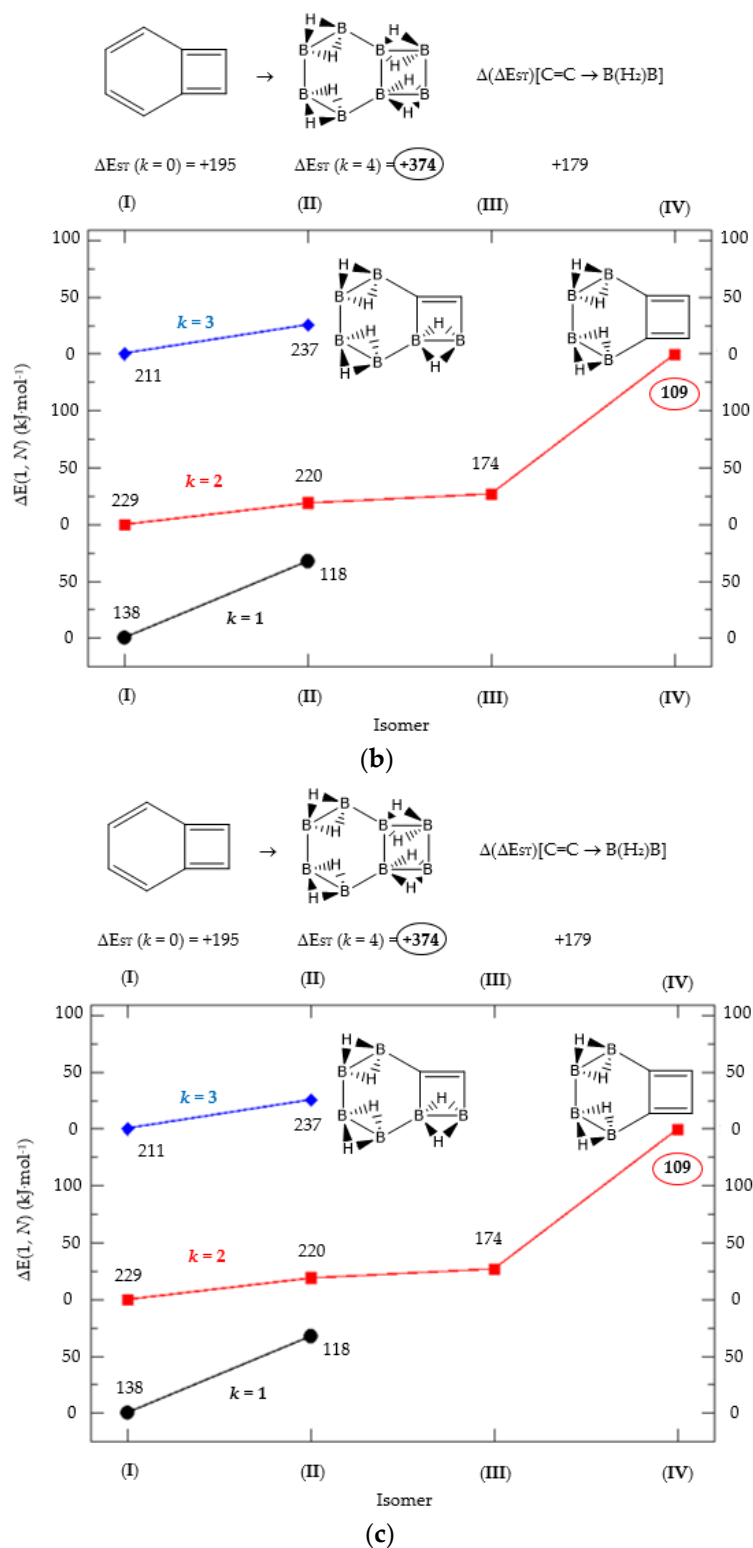


Figure 3. (a) Isomer structure vs. $\Delta E(I, N_{iso})$ (kJ·mol⁻¹) for benzocyclobutadiene Kekulé structure K_1 , with $\Delta E(I, N_{iso}) = E(N_{iso}) - E(I)$. (b) Isomer structure vs. $\Delta E(I, N_{iso})$ (kJ·mol⁻¹) for benzocyclobutadiene Kekulé structure K_2 . (c) Isomer structure vs. $\Delta E(I, N_{iso})$ (kJ·mol⁻¹) for benzocyclobutadiene Kekulé structure K_3 . N_{iso} is the number of isomers for a given k in $C_{(n-2k)}B_{(2k)}H_{(m+2k)}$. In addition, for each structure the singlet-triplet gap is shown (kJ·mol⁻¹). The encircled singlet-triplet gaps correspond to the maximum and minimum values.

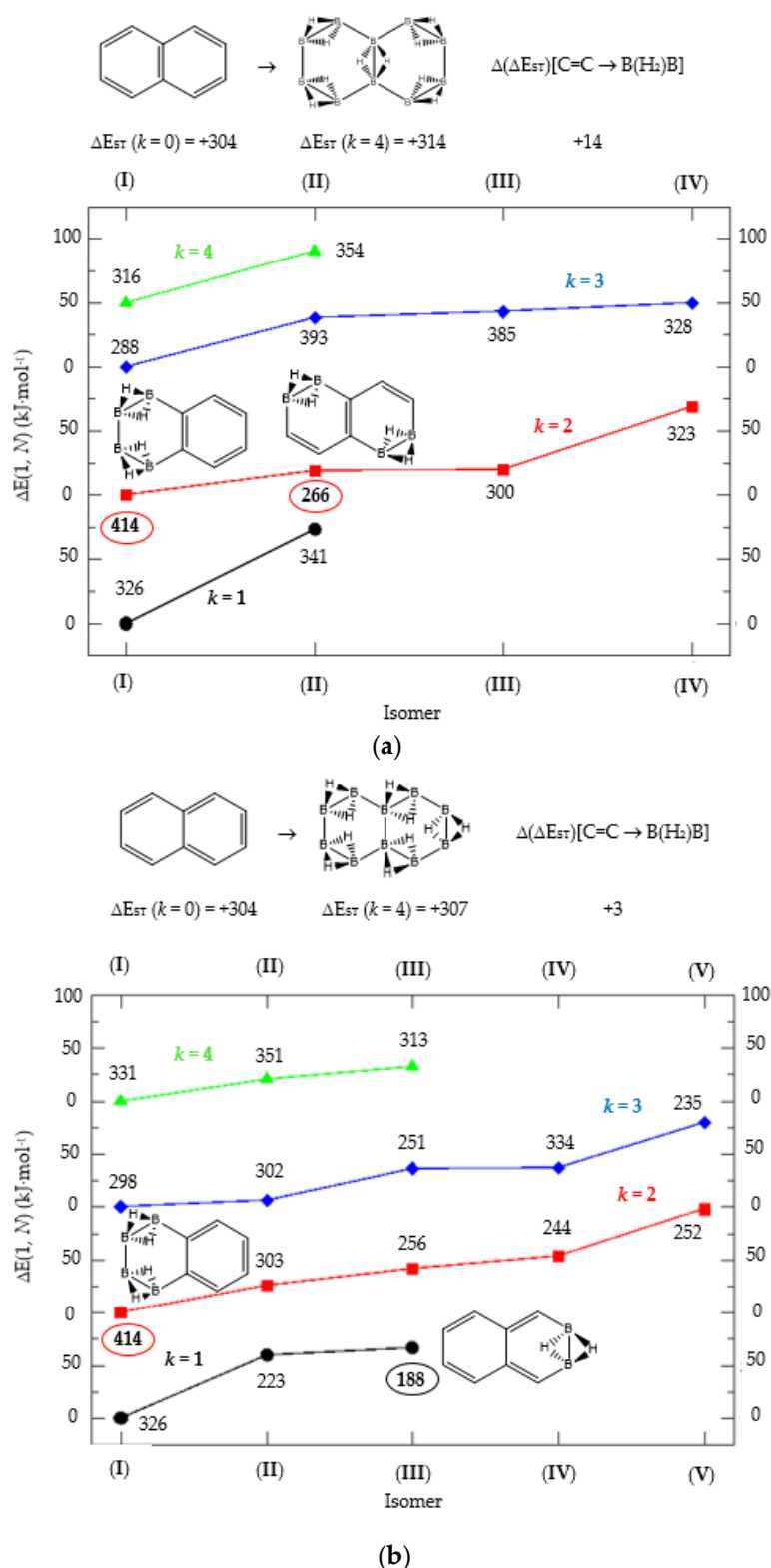


Figure 4. (a) Isomer structure vs. $\Delta E(I, N_{iso})$ ($\text{kJ}\cdot\text{mol}^{-1}$) for naphthalene Kekulé structure K_1 , with $\Delta E(I, N_{iso}) = E(N_{iso}) - E(I)$. (b) Isomer structure vs. $\Delta E(I, N)$ ($\text{kJ}\cdot\text{mol}^{-1}$) for naphthalene Kekulé structure K_2 . N_{iso} is the number of isomers for a given k in $C_{(n-2k)}B_{(2k)}H_{(m+2k)}$. In addition, for each structure the singlet-triplet gap is shown ($\text{kJ}\cdot\text{mol}^{-1}$). The encircled singlet-triplet gaps correspond to the maximum and minimum values.

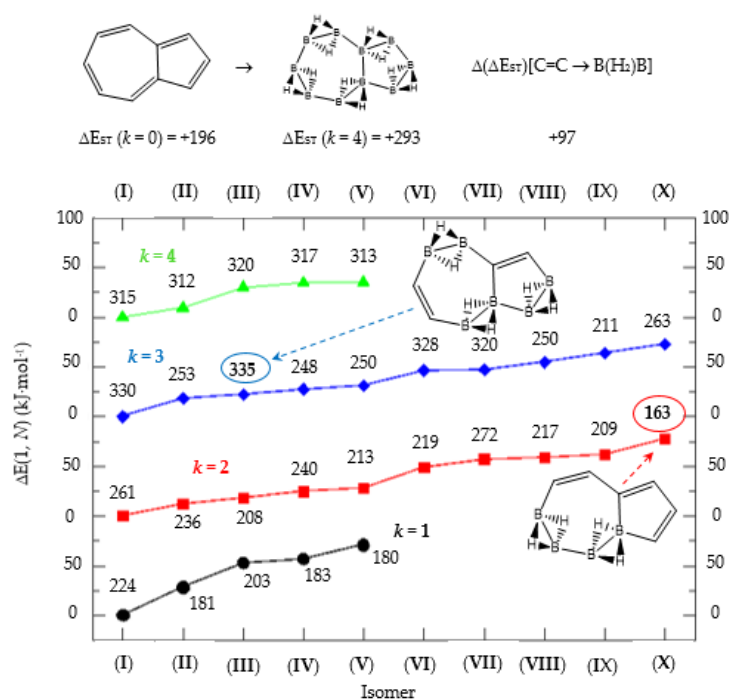


Figure 5. Isomer structure vs. $\Delta E(I, N_{iso})$ ($\text{kJ}\cdot\text{mol}^{-1}$) for azulene, with $\Delta E(I, N_{iso}) = E(N_{iso}) - E(I)$. N_{iso} is the number of isomers for a given k in $C_{(n-2k)}B_{(2k)}H_{(m+2k)}$. In addition, for each structure the singlet-triplet gap is shown ($\text{kJ}\cdot\text{mol}^{-1}$). The encircled singlet-triplet gaps correspond to the maximum and minimum values.

In order to highlight the electronic structure differences in benzene and its borane hybrids we have plotted in Table 1 the molecular electrostatic potential (MEP) for the benzene series $C_{(6-2k)}B_{(2k)}H_{(6+2k)}$, with $k = \{0, 1, 2, 3\}$: The blue and red colors in the MEP indicate negative and positive charge attraction areas: clearly, the benzene π -electron cloud is a positive-charge attraction area [29,30] and the borane substituted areas are negative-charge attraction areas, with a complete blue area above the boron-atoms plane in cyclic hexaborane(12) B_6H_{12} . Just below the MEP in Table 1 we show the anisotropy of the induced current density (ACID) [31] for the same systems, with a clear blocking of the current in the region where a $\{C=C \leftrightarrow B(H_2)B\}$ substitution is carried out; therefore π electron delocalization lowers considerably as k increases.

We turn now to an antiaromatic system with $n = 8 \pi$ electrons, cyclooctatetraene and the structural isoelectronic series summarized in Table 1 and Figure 1: $C_{(8-2k)}B_{(2k)}H_{(8+2k)}$, with $k = \{0, 1, 2, 3, 4\}$. Cyclooctatetraene is a colorless to light yellow flammable liquid at room temperature and adopts a non-planar D_{2d} structure in the ground state [32,33]. We should emphasize that cyclooctatetraene C_8H_8 ($k = 0$) and the corresponding borane equivalent B_8H_{16} ($k = 4$) are transition state structures in the planar D_{4h} conformation with energy barriers of $44.0 \text{ kJ}\cdot\text{mol}^{-1}$ [34] and $55.8 \text{ kJ}\cdot\text{mol}^{-1}$ respectively (B3LYP/cc-pVTZ computations), and thus the barrier for the $D_{2d} \rightarrow D_{4h}$ process is larger for the borane compound. Both energy minima correspond to D_{2d} structures, and this is the only series of non-planar hydrocarbon and hybrid boron-carbon structures included in this work. The main purpose of including cyclooctatetraene is due to the non-planarity of the system, which was not considered before [21].

Consecutive $\{C=C \leftrightarrow B(H_2)B\}$ substitutions in cyclooctatetraene C_8H_8 ($k = 0$) leads to $C_{(6-2k)}B_{(2k)}H_{(6+2k)}$ structures with a larger singlet-triplet energy gap as k increases from zero to 4, with a final gap which is $170 \text{ kJ}\cdot\text{mol}^{-1}$ larger as compared to the original hydrocarbon. Cyclooctatetraene is the first instance where we have two different positional isomers in $C_4B_4H_{12}$ ($k = 2$): Isomers I and II, with lower energy and larger singlet-triplet gap for the more symmetric structure I with C_{2v} symmetry. We define N_{iso} as the number of isomers for a given k in $C_{(n-2k)}B_{(2k)}H_{(m+2k)}$. For instance, for azulene

and $k = 2$ —see Table 5 below, we have a set of ten $C_6B_4H_{12}$ isomers: {**I**, **II**, **III**, ..., N_{iso} }, with $N_{iso} = 10$ in Roman numerals, i.e., $N_{iso} = X$.

We consider next the pentalene molecule C_8H_6 , a two-pentagon one-side fused conjugated system, also with $n = 8 \pi$ electrons, and therefore antiaromatic. Pentalene dimerizes at 173 K [35], and its derivative, 1,3,5-tri-tert-butylpentalene, has been synthesized [36], as a stabilized planar 8π electron system. In Table 2 and Figure 2 we gather the results for the pentalene series: $C_{(8-2k)}B_{(2k)}H_{(6+2k)}$, with $k = \{0, 1, 2, 3, 4\}$. Again, due to the antiaromatic nature of the hydrocarbon, the singlet-triplet energy gap in the equivalent boron structure ($k = 4$) is $157 \text{ kJ}\cdot\text{mol}^{-1}$ higher in energy, as in the previous antiaromatic cases for cyclobutadiene and cyclooctatetraene, and the energy gap in pentalene is the lowest along the whole series of structures and isomers derived from $C_{(8-2k)}B_{(2k)}H_{(6+2k)}$ and $1 < k \leq 4$, as the encircled value shown at the top of Figure 2.

The singlet-triplet energy gaps increase along the series for $0 \leq k \leq 3$; the equivalent boron structure B_8H_{14} ($k = 4$) has a lower gap as compared to the previous ($k = 3$) molecule $C_2B_6H_{12}$. There are striking differences in the energy gaps as function of k , the number of $\{C=C \leftrightarrow B(H_2)B\}$ substitutions, and also within the set of isomers of a given k , as shown in Figure 2. The largest and lowest singlet-triplet energy gaps in the whole series are shown in Figure 2 as encircled numbers and with the corresponding structure. All structures and isomers for $1 \leq k \leq 4$ have a larger singlet-triplet energy gap as compared to original pentalene ($k = 0$), a clear indication on how unstable this conjugated hydrocarbon is as compared to the boron-carbon hybrid series.

As shown in Table 2 and Figure 2 the isomer energies for a given structure (k) follow the same order as the singlet-triplet gaps, except isomer **IV** for $k = 2$ with an increase of $100 \text{ kJ}\cdot\text{mol}^{-1}$. It is striking that isomers with very close electronic energies might have such different singlet-triplet gaps. The energy difference between isomers **III** and **IV** for $k = 2$ is only $7 \text{ kJ}\cdot\text{mol}^{-1}$. Hence positional $\{C=C \leftrightarrow B(H_2)B\}$ substitutions might have important changes in the interaction of these hybrid boron-carbon isomers with external perturbations, such as photochemical processes.

We follow with another conjugated hydrocarbon with $n = 8 \pi$ electrons: benzocyclobutadiene and the hybrid boron-carbon series $C_{(8-2k)}B_{(2k)}H_{(6+2k)}$, with $k = \{0, 1, 2, 3, 4\}$, similar to pentalene, and displayed in Table 3a–c and Figure 3a–c. Benzocyclobutadiene polymerises readily and reacts as a dienophile in Diels-Alder reactions [37]. As opposed to the previous $n = 8$ systems, in this particular case we need to consider different Kekulé structures, K_1 , K_2 and K_3 (Scheme 1) since they give different structural isomers on consecutive $k \{C=C \leftrightarrow B(H_2)B\}$ substitutions. The energy gap in the original hydrocarbon is $195 \text{ kJ}\cdot\text{mol}^{-1}$ (the same for K_1 , K_2 and K_3) and we find for the first time that $\{C=C \leftrightarrow B(H_2)B\}$ substitutions lead to hybrid systems with lower gaps, e.g., isomer **IV** with $k = 2$ in Table 3a with a gap of $108 \text{ kJ}\cdot\text{mol}^{-1}$, the lowest among all as shown in Figure 3a, clearly due to the presence of the strained cyclobutadiene ring in the structure. Only isomers from Kekulé structures K_1 and K_3 keep this tendency as shown in Table 3a–c respectively. There is an exception to this behavior: for the Kekulé structure K_2 —Table 3b—the gaps are always larger in the substituted isomers, as compared to benzocyclobutadiene. This is striking and due to the presence of only one double bond $C=C$ in the rectangular cyclobutadiene, hence lowering the strain energy on any further $\{C=C \leftrightarrow B(H_2)B\}$ substitution. Another noteworthy result is the singlet-triplet energy gap differences in the boron equivalent structures of K_1 , K_2 and K_3 , always fairly above benzocyclobutadiene by $70 \text{ kJ}\cdot\text{mol}^{-1}$, $115 \text{ kJ}\cdot\text{mol}^{-1}$ and $180 \text{ kJ}\cdot\text{mol}^{-1}$ respectively, as shown in Figure 3a–c.

There are many isomers with larger energy gaps as compared to benzocyclobutadiene: The borane structure for planar ($k = 4$) B_8H_{14} in the K_3 configuration—Table 3c and Figure 3c—has the largest gap of all structures and isomers, $374 \text{ kJ}\cdot\text{mol}^{-1}$. When strain is released from the rectangular cyclobutadiene moiety in the original hydrocarbon, many isomers have gaps above $300 \text{ kJ}\cdot\text{mol}^{-1}$, with the interesting case of isomer **I** of K_2 with $k = 2$ —Table 4b—a *cis*-butadiene system fused with two diborane molecules and energy gap $368 \text{ kJ}\cdot\text{mol}^{-1}$ and the lowest ground state energy. The experimental vertical singlet-triplet gap in butadiene is $310.7 \text{ kJ}\cdot\text{mol}^{-1}$ [38] ($318.9 \text{ kJ}\cdot\text{mol}^{-1}$ with a B3LYP/cc-pVTZ computation). Therefore, the two diborane molecules fused to the *cis*-butadiene moiety in isomer **I**

of $C_4B_4H_{10}$ ($k = 2$) and Kekulé structure K_2 stabilise the system further by $50 \text{ kJ}\cdot\text{mol}^{-1}$. We do not intend to give spectroscopic accuracy in these examples, but rather an explanation of the tendency in energy and stability changes upon $\{C=C \leftrightarrow B(H_2)B\}$ substitutions in conjugated hydrocarbons. We should emphasize here that all structures and isomers remain planar upon these substitutions in benzocyclobutadiene, checked through frequency computations, thus following the previous examples with the exception of cyclooctatetraene, which is not planar.

Given the topological distribution of single and double bonds in benzocyclobutadiene, only Kekulé structures K_1 and K_3 retain the cyclobutadiene ring in the hybrid boron-carbon series. Hence, for K_1 —Table 3a and Figure 3a—one has isomer **III** from $C_6B_2H_8$ ($k = 1$), with an energy gap of $118 \text{ kJ}\cdot\text{mol}^{-1}$ and isomer **IV** from $C_4B_6H_{10}$ ($k = 2$) with a gap of $108 \text{ kJ}\cdot\text{mol}^{-1}$ (lowest gap). These isomers are equivalent in K_3 —Table 3c and Figure 3c—to isomer **II** from $C_6B_2H_8$ ($k = 1$), and isomer **IV** from $C_4B_6H_{10}$ ($k = 2$). The presence of the cyclobutadiene ring explains why these hybrid boron-carbon isomers have such low singlet-triplet energy gaps.

We turn now to the next aromatic system, naphthalene, with $n = 10 \pi$ electrons, and the series $C_{(10-2k)}B_{(2k)}H_{(8+2k)}$, with $k = \{0, 1, 2, 3, 4\}$. Naphthalene is a white crystalline solid with a characteristic odor and detectable at very low concentrations and reacts more readily than benzene in electrophilic aromatic substitution reactions [37]. The two Kekulé structures K_1 and K_2 shown in Scheme 1 are also necessary in order to include all possible different isomers upon consecutive $\{C=C \leftrightarrow B(H_2)B\}$ substitutions. Table 4a,b and Figure 4a,b include the energies and energy gaps for all isomers derived from Kekulé structures K_1 and K_2 in naphthalene, respectively. What differs notably, *viz.*, the energy gaps as compared to antiaromatic systems ($n = 4, 8$)—see above also benzene—is the small difference between the gaps in the original conjugated hydrocarbon $C_{10}H_8$ and the equivalent borane structure $B_{10}H_{18}$, $10 \text{ kJ}\cdot\text{mol}^{-1}$ and $3 \text{ kJ}\cdot\text{mol}^{-1}$ higher for Kekulé structures K_1 and K_2 respectively. Therefore, from a thermochemical point of view, the synthesis of the planar borane structures derived from benzene and naphthalene, B_6H_{12} and $B_{10}H_{18}$ respectively, should be affordable.

Again, for an aromatic system, consecutive $\{C=C \leftrightarrow B(H_2)B\}$ substitutions lead to larger energy gaps compared to naphthalene, with a striking increase for the $k = 2$ isomer **I** in structures K_1 and K_2 —both are equivalent— $C_6B_4H_{12}$ ($k = 2$)—Table 4a—which corresponds to a fusion of two diborane molecules to benzene, and giving a further stability to the molecule. Isomers with lower gaps than naphthalene appear both in K_1 and K_2 structures. The two lowest gaps in K_1 correspond to isomers **II** from $C_6B_4H_{12}$ ($k = 2$) and isomer **I** from $C_4B_6H_{14}$ ($k = 3$). The lowest gap in K_2 —Table 4b—correspond to the $k = 1$ isomer **III** from structure $C_8B_2H_{10}$; this destabilisation is clearly due to the loss of aromaticity in the whole system on substituting one $C=C$ bond by a $B(H_2)B$ moiety on the right ending of the molecule, thus quenching the resonance energy.

We should also emphasize that K_1 set has more isomers than the K_2 set with a gap larger than naphthalene, and all isomers are planar structures corresponding to energy minima for all set of Kekulé structures.

Finally, the last system included in this work, aromatic azulene with $n = 10 \pi$ electrons follows the same series as in naphthalene: $C_{(10-2k)}B_{(2k)}H_{(8+2k)}$, with $k = \{0, 1, 2, 3, 4, 5\}$. Two terpenoids of azulene appear in Nature and offer a rich organic chemistry [39]. In azulene we have one, 5 and 10 isomers for $k = \{0, 5\}$, $k = \{1, 4\}$ and $k = \{2, 3\}$ respectively, as shown in Table 5 and Figure 5. There is only one Kekulé structure leading to different isomers, and the presence of a seven-membered ring fused to a five-membered ring entails a different electronic structure as depicted by the lower energy gap in the original hydrocarbon as compared to benzene and naphthalene.

The azulene equivalent borane structure $B_{10}H_{18}$ has a singlet-triplet energy gap $100 \text{ kJ}\cdot\text{mol}^{-1}$ above the original system and again there are isomers with lower and higher energy gaps as compared to azulene. The largest and lowest gaps correspond to $335 \text{ kJ}\cdot\text{mol}^{-1}$ and $163 \text{ kJ}\cdot\text{mol}^{-1}$ for isomer **III** of structure $C_4B_6H_{14}$ ($k = 3$) and isomer **X** of structure $C_6B_4H_{12}$ ($k = 2$), respectively, as displayed in Figure 5, with the encircled numbers. The general rule is that the average gap increases with k for $1 < k < 4$, namely, the more $\{C=C \leftrightarrow B(H_2)B\}$ substitutions, the more stable the system on average.

One $\{C=C \leftrightarrow B(H_2)B\}$ substitution in azulene, leading to five $C_8B_2H_{10}$ isomers ($k = 1$), shows two isomers (I, III) with an energy gap above azulene and three isomers (II, IV and V) with energy gaps below azulene. The energy gap in isomer III is only $4 \text{ kJ}\cdot\text{mol}^{-1}$ higher than in azulene. Note that the structural difference between isomer I and isomer V of structure $C_8B_2H_{10}$ ($k = 1$) stems from the boron substitution site: pentagon and heptagon respectively, and both on the bridge atomic site. Boron substitution on the pentagon cycle at the bridge position leads to the least reactive species ($k = 1$) $C_8B_2H_{10}$ (I) as compared to azulene. However, this situation is inverted when the boron substitution site is on the bridge position of the heptagon cycle, leading to the more reactive isomer V for $C_8B_2H_{10}$ ($k = 1$) as compared to azulene. As commented above, complete boron substitution of azulene ($k = 4$) leads to a more stable structure, with a singlet-triplet gap $100 \text{ kJ}\cdot\text{mol}^{-1}$ above azulene. This is remarkable if we take into account that $B_{10}H_{18}$ has never been synthesized.

3. Discussion

The experimental CC and BB distances in ethylene and diborane(6) are 1.340 \AA and 1.736 \AA respectively. These are considerable differences which are due mainly to the presence of two bridge hydrogen atoms in diborane(6), changing the electronic structure of the substituted systems considerably. However, the role of these two bridge hydrogen atoms in the $B(H_2)B$ moiety correspond, from a structural and electronic point of view, to the two π electrons in ethylene: Every $\{C=C \leftrightarrow B(H_2)B\}$ substitution in the original conjugated C_nH_m hydrocarbon leads to a hybrid planar or nonplanar equivalent structure, as we have seen above in the description of the results. The aromaticity and antiaromaticity of a conjugated C_nH_m system according to Hückel's $4n + 2$ and $4n$ rule for π electrons, respectively, does not necessarily apply by consecutive $\{C=C \leftrightarrow B(H_2)B\}$ substitutions, leading to the hybrid systems $C_{(n-2k)}B_{(2k)}H_{(m+2k)}$, with $k = \{0, 1, 2, \dots, n/2\}$. The geometrical parameters for cyclobutadiene, benzene and cyclooctatetraene and the hybrid boron-carbon systems are gathered in Table 6.

According to Table 6, inclusion of empirical dispersion corrections in the B97D functional leads to slightly larger distances in a systematic way as compared to the B3LYP results, without changing the minimum energy nature of the stationary points for the conjugated hydrocarbon structures and the corresponding boron-carbon hybrids.

As regards to the singlet-triplet energy gaps in the same three model systems, we gathered in Table 1 the B3LYP and B97D energy gaps, with a systematic lowering when including dispersion corrections, and following the same trend; since our goal here is a tentative prediction, from a theoretical point of view, of the stabilities in hybrid boron-carbon systems which are experimentally unknown, the qualitative description is valid, without pretending spectroscopic accuracy.

A further assessment on the degree of aromaticity in the hybrid boron-carbon systems included in this work can be tackled with the comparison of the nucleus-independent chemical shifts (NICS) [40], at the centre of ring—NICS(0)—and 1 \AA above this point, perpendicular to the ring—NICS(1). NICS is a computational method which provides the extent of absolute magnetic shielding at the centre of a ring. The values are reported with a reversed sign to make them compatible with the chemical shift conventions of NMR spectroscopy, and negative NICS values indicate aromaticity and positive values antiaromaticity. In Table 7 we gather the NICS(0) and NICS(1) values for cyclobutadiene and benzene with the corresponding hybrids.

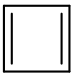
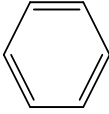
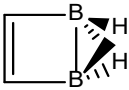
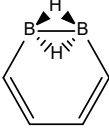
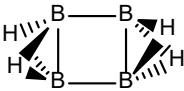
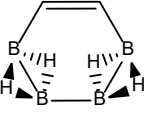
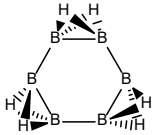
Cyclobutadiene is the most antiaromatic system, and the NICS values decrease with more $\{C=C \leftrightarrow B(H_2)B\}$ substitutions. Clearly, benzene is the most aromatic system considered here and the first hybrid with one $\{C=C \leftrightarrow B(H_2)B\}$ substitution retains certain degree of aromaticity. A further $\{C=C \leftrightarrow B(H_2)B\}$ substitution leads to a positive NICS(0) and a small negative NICS(1). Complete $\{C=C \leftrightarrow B(H_2)B\}$ substitutions in benzene leads to a non-aromatic cyclic hexaborane(12) B_6H_{12} . The ACID plots (Table 1) of the benzene derivatives show that each $\{C=C \leftrightarrow B(H_2)B\}$ substitution produces gaps in the isosurface as indication of reduced aromaticity. In Figure 6 we display the

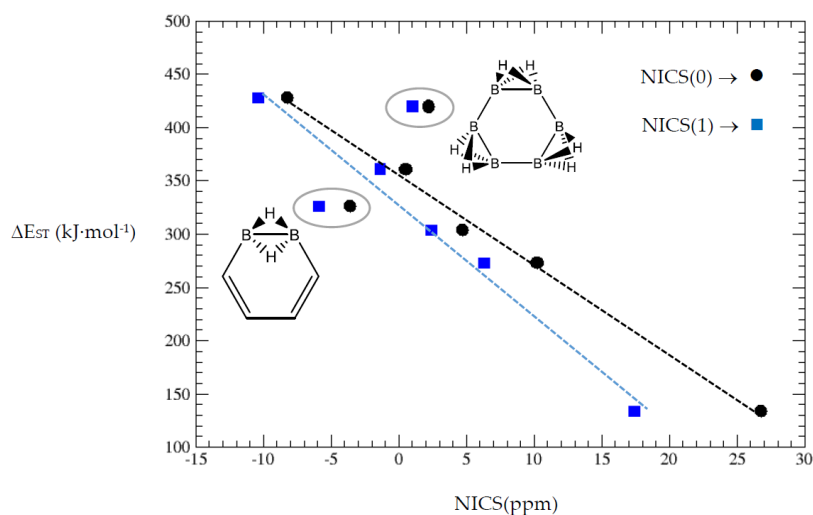
correlation between the singlet-triplet energy gap vs. NICS(0) and NICS(1) from Table 7. The correlations are quite linear except for the two encircled hybrid structures.

Table 6. Geometrical distances (Å) in optimised geometries of $C_{(n-2k)}B_{(2k)}H_{(m+2k)}$ systems for cyclobutadiene, benzene and cyclooctatetraene: $d(C-C)$, $d(C=C)$, $d(C-H)$, $d(B-B)$, $d(B(H_b)_2B)_b$, $d(B-H)$, and $d(H_b-H_b)$. H_b corresponds to a bridge hydrogen atom, i.e., diborane(6) can be drawn as $H_2B(H_b)_2BH_2$. The first and second (italic) value for each distance corresponds respectively to B3LYP/cc-pVTZ and B97D/cc-pVTZ computations, the latter with a functional including dispersion corrections.

	$d(C-C)$	$d(C=C)$	$d(C-H)$	$d(B-B)$	$d(B(H_b)_2B)$	$d(B-H)$	$d(H_b-H_b)$
Ethylene	—	1.324 1.332	1.083 1.089	—	—	—	—
Diborane(6)	—	—	—	—	1.758 1.777	1.185 1.195	1.948 1.973
Cyclobutadiene (<i>k</i>)	$d(C-C)$	$d(C=C)$	$d(C-H)$	$d(B-B)$	$d(B(H_b)_2B)$	$d(B-H)$	$d(H_b-H_b)$
C_4H_4 (0)	1.575 1.582	1.329 1.337	1.079 1.085	—	—	—	—
$C_2B_2H_6$ (1)	—	1.338 1.347	1.083 1.09	—	1.741 1.749	1.185 1.194	1.858 1.886
B_4H_8 (2)	—	—	—	1.728 1.739	1.76 1.771	1.189 1.199	1.856 1.883
Benzene (<i>k</i>)	$d(C-C)$	$d(C=C)$	$d(C-H)$	$d(B-B)$	$d(B(H_b)_2B)$	$d(B-H)$	$d(H_b-H_b)$
C_6H_6 (0)	1.391 1.399	1.391 1.399	1.082 1.087	—	—	—	—
$C_4B_2H_8$ (1)	1.439 1.442	1.359 1.369	1.085 1.09	—	1.799 1.823	1.186 1.196	1.926 1.951
$C_2B_4H_{10}$ (2)	—	1.35 1.359	1.088 1.094	1.695 1.708	1.789 1.812	1.188 1.198	1.926 1.952
B_6H_{12} (3)	—	—	—	1.713 1.724	1.793 1.812	1.19 1.2	1.923 1.948
Cyclooctatetraene (<i>k</i>)	$d(C-C)$	$d(C=C)$	$d(C-H)$	$d(B-B)$	$d(B(H_b)_2B)$	$d(B-H)$	$d(H_b-H_b)$
C_8H_8 (0)	1.469 1.471	1.335 1.343	1.087 1.092	—	—	—	—
$C_6B_2H_{10}$ (1)	1.47 1.471	1.338 1.347	1.088 1.093	—	1.77 1.788	1.191 1.202	1.944 1.972
$C_4B_4H_{12}$ (2) (I)	—	1.341 1.349	1.09 1.096	—	1.785 1.804	1.19 1.202	1.94 1.966
$C_4B_4H_{12}$ (2) (II)	1.475 1.476	1.34 1.348	1.089 1.095	1.694 1.706	1.776 1.791	1.191 1.202	1.941 1.969
$C_2B_6H_{14}$ (3)	—	1.343 1.351	1.091 1.096	1.696 1.706	1.777 1.796	1.191 1.202	1.938 1.964
B_8H_{16} (4)	—	—	—	1.698 1.708	1.786 1.8	1.191 1.202	1.934 1.96

Table 7. NICS(0) and NICS(1), in ppm for cyclobutadiene and benzene and the corresponding hybrids.

Cyclobutadiene	NICS(0)	NICS(1)	Benzene	NICS(0)	NICS(1)
	26.8	17.4		-8.2	-10.4
	10.2	6.3		-3.6	-5.9
	4.7	2.4		0.5	-1.4
				2.2	1.0

**Figure 6.** Singlet-triplet energy gaps vs. NICS(0) and NICS(1) for cyclobutadiene and benzene series.

The most noticeable changes upon $\{C=C \leftrightarrow B(H_2)B\}$ substitutions for a given conjugated hydrocarbon C_nH_m , from an energy point of view and singlet-triplet gap, is in the loss of aromaticity or in the inclusion or permanence of very unstable moieties, such as cyclobutadiene. For instance, for antiaromatic cyclobutadiene and cyclooctatetraene—Table 1 and Figure 1—the minimum and maximum singlet-triplet energy gaps correspond respectively to the conjugated hydrocarbon C_nH_m and the corresponding borane systems B_nH_{m+n} respectively, namely, with all $k = n/2$ $\{C=C \leftrightarrow B(H_2)B\}$ substitutions. This is remarkable, since planarity of borane molecules is an exception rather a rule. The loss of aromaticity in benzene upon one $\{C=C \leftrightarrow B(H_2)B\}$ substitution leads to the minimum energy gap structure, with the largest gap for benzene itself. Pentalene has the lowest energy gap as shown in Table 2 and Figure 2, as an antiaromatic system, with the larger gap for the $k = 3$ isomer (I), where only one $C=C$ double bond remains in the structure, releasing the constrained hydrocarbon structure due to longer BB and $B(H_b)_2B$ distances. The particular case of benzocyclobutadiene, also antiaromatic, is remarkable due to the three different Kekulé structures leading to different isomers, Table 3a–c and Figure 3a–c. Thus, for K_1 , the minimum singlet-triplet gap comes from the $k = 2$, isomer (IV), which is nothing but a cyclobutadiene molecule with two diborane(6) moieties attached

to one of the C=C double bonds forming a six-member cycle: This isomer has a gap which is even lower than in cyclobutadiene itself! On the other hand, and following the cases of cyclobutadiene and cyclooctatetraene, the complete borane structure ($k = 4$) B_6H_{14} has the largest gap. For Kekulé structure K_2 , benzocyclobutadiene itself has the lowest gap and the largest gap corresponds to $k = 2$ isomer (I), a *cis*-butadiene molecule with two diborane(6) molecules fused and forming a six- and four-member ring on the =CH₂ and =CH- moieties respectively. Hence the conjugation of the two double bonds is maintained even with the inclusion of diborane moieties. As for K_3 , the minimum gap corresponds to the $k = 2$ isomer (IV) which is cyclobutadiene with two fused diborane molecules forming a six-member ring; note that whenever a cyclobutadiene is maintained in the {C=C ↔ B(H₂)B} substitutions the energy gap is very, thus predicting a very reactive system. Again, the maximum energy gap corresponds the completed borane structure with four {C=C ↔ B(H₂)B} substitutions: This is a rule for antiaromatic systems.

We now turn to aromatic naphthalene with the K_1 and K_2 Kekulé structures as displayed in Table 4a–b and Figure 4a,b. Due to the indistinguishable nature of the two valence-bond Kekulé structures in benzene, the $k = 2$ isomer (I) is equivalent for K_1 and K_2 and corresponds to a benzene molecule with two diborane molecules fused forming an additional six-member ring. If we use a valence-bond or multiconfigurational wave function, these isomers would have a different energy due to the different spin-coupling patterns. In our approximation, this isomer has the largest energy gap due to the aromaticity of benzene, which is only 14 kJ·mol⁻¹ higher than in benzene. The lowest energy gaps correspond to structures where the cyclic aromaticity is somehow broken due to {C=C ↔ B(H₂)B} substitutions in concrete places: for K_1 this corresponds to $k = 2$ isomer (II), with three consecutive C=C bonds passing through the bridge C=C bond but with two B(H₂)B moieties on opposite rings, thus destroying the cyclic aromaticity. As for K_2 , the lowest gap corresponds to the $k = 1$ isomer (III) and similarly the aromaticity is destroyed by one {C=C ↔ B(H₂)B} substitution on the ending edge. We should emphasize that in this latter case the energy gap is much lower as compared to the minimum gap structure for K_1 since the three consecutive alternating C=C bonds gives further stability of the $k = 2$ isomer (II) structure.

Finally, azulene boron-carbon hybrids give a range of singlet-triplet gaps from 163 kJ·mol⁻¹ to 335 kJ·mol⁻¹, corresponding to structures $k = 2$ isomer (X) and $k = 3$ isomer (III) respectively, as shown in Table 5 and Figure 5. Due to the larger seven-member ring the structures are less constrained, but the presence of a cyclopentadiene ring lowers the stability. The lowest energy gap structure— $k = 2$ isomer (X)—consists of a cyclopentadiene ring where one of the connecting atoms is a boron atom; this structure should be very reactive indeed.

4. Computational Methods

The quantum-chemical computations of the structures and isomers included in this work were carried out with the B3LYP/cc-pVTZ model [41–44] and with the scientific software Gaussian16 [45]. All geometries correspond to energy minima, checked through frequency computations, with geometry optimisation thresholds of 0.00045 Hartree/Bohr and 0.00030 Hartree/Bohr for maximum force and root-mean-square (RMS) force respectively, and 0.0018 Bohr and 0.0012 Bohr for maximum displacement and RMS displacement respectively. For the computations of the $D_{2d} \rightarrow D_{4h}$ barriers in cyclooctatetraene C_8H_8 and the boron substituted system B_8H_{16} , the optimized geometries showed zero and one imaginary frequency for the D_{2d} and D_{4h} geometries, respectively. The MEP and ACID plots for benzene and the $C_{(6-2k)}B_{(2k)}H_{(6+2k)}$ series, $k = \{1-3\}$ (Table 1), were also computed with Gaussian16.

5. Conclusions

The goal of this work was to check the structural stability from any conjugated hydrocarbon C_nH_m through the boron-carbon hybrid series $C_{(n-2k)}B_{(2k)}H_{(m+2k)}$, obtained upon k {C=C ↔ B(H₂)B} substitutions for $k = \{0, 1, 2, \dots, n/2\}$, leading to the structurally equivalent complete borane B_nH_{m+n} structure, for $k = n/2$. We have chosen planar and non-planar conjugated hydrocarbons: cyclobutadiene

($n = 4$), benzene ($n = 6$), cyclooctatetraene ($n = 8$), pentalene ($n = 8$), naphthalene ($n = 10$) and azulene ($n = 10$). As a result, all hybrid boron-carbon structures appear as energy minima from the quantum-chemical computations and therefore, from a thermodynamic point of view, they should be a synthetic target for experimentalists working on planar boron chemistry. This is unusual if we consider that borane polyhedral molecules are 3D curved structures. In the particular case of cyclooctatetraene C_8H_8 , a non-planar structure, we have shown that the one-to-one structural equivalence $C_nH_m \leftrightarrow B_nH_{m+n}$ also holds; the energy barrier for loss of planarity from a planar transition state structure (D_{4h}) to an energy minimum twisted structure (D_{2d}) is larger for the cyclic borane B_8H_{16} , as compared to cyclic octatetraene. Structural isomers appear for a given number k of $\{C=C \leftrightarrow B(H_2)B\}$ substitutions in an isoelectronic series $C_{(n-2k)}B_{(2k)}H_{(m+2k)}$ with $k = \{0, 1, 2, \dots, n/2\}$ for all conjugated hydrocarbons, except for cyclobutadiene and benzene, with a maximum number of isomers of 10 for azulene structures with $C_6B_4H_{12}$ ($k = 2$) and $C_4B_6H_{14}$ ($k = 3$) formulae. These isomers are ordered in increasing energy $\{I, II, \dots, N_{iso}\}$. Striking energy differences in an isomeric series stem from one $\{C=C \leftrightarrow B(H_2)B\}$ substitution in the cyclobutadiene cycle from benzocyclobutadiene with an energy jump of $125 \text{ kJ}\cdot\text{mol}^{-1}$. As regards to the energy order of vertical singlet-triplet energy gaps, they do not necessarily follow the same trend as compared to the energy profile for the isomers of a given k in a $C_{(n-2k)}B_{(2k)}H_{(m+2k)}$ structure.

The vertical singlet-triplet energy gaps in conjugated hydrocarbons C_nH_m vs. B_nH_{m+n} change strikingly in antiaromatic systems, when the number of π electrons is $4n$, with the energy gap always much larger for the borane systems. On the other hand, for conjugated hydrocarbons with $(4n + 2)$ electrons—Hückel rule for aromaticity—the difference in vertical singlet-triplet energy gaps between C_nH_m and B_nH_{m+n} is minor for benzene and naphthalene and larger for azulene. From these results a potential rule arises, which will be thoroughly checked in a future work and holds for the systems included here: the lowest and largest singlet-triplet energy gap for a $C_{(n-2k)}B_{(2k)}H_{(m+2k)}$ series of structures—with n multiple of 4—always corresponds to the $k = 0$ and $k = n/2$ structure respectively, namely, to the original conjugated hydrocarbon C_nH_m and the complete borane structure B_nH_{m+n} . We should also emphasize that, if aromatic structures—e.g., π sextets in six-member rings—are maintained in a given isoelectronic $C_{(n-2k)}B_{(2k)}H_{(m+2k)}$ series, then the singlet-triplet energy gap is large and similar to the original conjugated hydrocarbon and the structure is predicted to be stable. On the other hand, the presence of an antiaromatic structure—e.g., cyclobutadiene moieties with 4π electrons—in any $C_{(n-2k)}B_{(2k)}H_{(m+2k)}$ system, lowers considerably the energy gap thus predicting an unstable structure. Finally, the existence of similar structures derived from phenanthrene derivatives with one $\{C=C \leftrightarrow B(H_2)B\}$ substitution in the conjugated hydrocarbon [19–23], gives support to the possibility of synthesizing or characterizing the hybrid boron-carbon isoelectronic $C_{(n-2k)}B_{(2k)}H_{(m+2k)}$ structures presented in this work.

Supplementary Materials: B3LYP/cc-pVTZ optimised geometries, in cartesian coordinates (Å), of the systems included in the work.

Author Contributions: Conceptualization, J.M.O.-E., I.A. and J.E., writing—review and editing J.M.O.-E., I.A. and J.E. All authors have read and agreed to the published version of the manuscript.

Funding: This research was funded by Spanish MICINN, grant number CTQ2018-094644-B-C22 and Comunidad de Madrid, grant number P2018/EMT-4329 AIRTEC-CM.

Conflicts of Interest: The authors declare no conflict of interest.

References

1. Hückel, E. Quantentheoretische Beiträge zum Benzolproblem. *Z. Phys.* **1931**, *70*, 204–286. [[CrossRef](#)]
2. Pauling, L. *The Nature of the Chemical Bond and the Structure of Molecules and Crystals*, 3rd ed.; Cornell University Press: Ithaca, NY, USA, 1960.
3. Heitler, W.; London, F. Wechselwirkung neutraler Atome und homöopolare Bindung nach der Quantenmechanik. *Z. Phys.* **1927**, *44*, 455–472. [[CrossRef](#)]
4. Hund, F. Zur Deutung einiger Erscheinungen in den Molekelspektren. *Z. Phys.* **1926**, *36*, 657. [[CrossRef](#)]

5. Mulliken, R.S. Electronic states and band spectrum structure in diatomic Molecules. I. Statement of the postulates. Interpretation of CuH, CH, and Co band-types. *Phys. Rev.* **1926**, *28*, 481. [[CrossRef](#)]
6. Woodward, R.B.; Hoffmann, R. Stereochemistry of electrocyclic reactions. *J. Am. Chem. Soc.* **1965**, *87*, 395–397. [[CrossRef](#)]
7. Kamtekar, K.T.; Monkman, A.P.; Bryce, M.R. Recent advances in white organic light-emitting materials and devices (WOLEDs). *Adv. Mater.* **2010**, *22*, 572–582. [[CrossRef](#)] [[PubMed](#)]
8. Shavitt, I. Geometry and singlet-triplet energy gap in methylene: A critical review of experimental and theoretical determinations. *Tetrahedron* **1985**, *41*, 1531–1542. [[CrossRef](#)]
9. Chutjian, A.; Hall, R.I.; Trajmar, S. Electron-impact excitation of H₂O and D₂O at various scattering angles and impact energies in the energy-loss range 4.2–12 eV. *J. Chem. Phys.* **1975**, *63*, 892–898. [[CrossRef](#)]
10. Stock, A. *The Hydrides of Boron and Silicon*; Cornell University Press: Ithaca, NY, USA, 1933.
11. Brown, H.C. From little acorns to tall oaks from boranes through organoboranes. In *Nobel Lecture, 8 December 1979*; World Scientific Publishing Co.: Singapore, 1993.
12. Marder, T.B.; Lin, Z. (Eds.) *Contemporary Metal Boron Chemistry I: Borylenes, Boryls, Borane Sigma-Complexes, and Borohydrides*; Springer: Berlin, Germany, 2008.
13. Lipscomb, W.N. *Boron Hydrides*; Dover Publications Inc.: Mineola, NY, USA, 2012.
14. Štibr, B. Carboranes other than C₂B₁₀H₁₂. *Chem. Rev.* **1992**, *92*, 225–250. [[CrossRef](#)]
15. Grimes, R.N. *Carboranes*, 3rd ed.; Academic Press: Cambridge, MA, USA, 2016.
16. Saxena, A.K.; Hosmane, N.S. Recent advances in the chemistry of carborane metal complexes incorporating d- and f-block elements. *Chem. Rev.* **1993**, *93*, 1081–1124. [[CrossRef](#)]
17. Poater, J.; Viñas, C.; Bennour, I.; Escayola, S.; Solà, M.; Teixidor, F. Too persistent to give up: Aromaticity in boron clusters survives radical structural changes. *J. Am. Chem. Soc.* **2020**, *142*, 9396–9407. [[CrossRef](#)] [[PubMed](#)]
18. Nishino, H.; Fujita, T.; Cuong, N.T.; Tominaka, S.; Miyauchi, M.; Iimura, S.; Hirata, A.; Umezawa, N.; Okada, S.; Nishibori, E.; et al. Formation and characterization of hydrogen boride sheets derived from MgB₂ by cation exchange. *J. Am. Chem. Soc.* **2017**, *139*, 13761–13769. [[CrossRef](#)] [[PubMed](#)]
19. Wrackmeyer, B.; Thoma, P.; Kempe, R.; Glatz, G. 9-Borafluorenes—NMR spectroscopy and DFT calculations. Molecular structure of 1,2-(2,2'-diphenyllylene)-1,2-diethyldiborane. *Collect. Czech. Chem. Commun.* **2010**, *75*, 743–756. [[CrossRef](#)]
20. Das, A.; Hübner, A.; Weber, M.; Bolte, M.; Lerner, H.-W.; Wagner, M. 9-H-9-Borafluorene dimethyl sulfide adduct: A product of a unique ring-contraction reaction and a useful hydroboration reagent. *Chem. Commun.* **2011**, *47*, 11339–11341. [[CrossRef](#)] [[PubMed](#)]
21. Hübner, A.; Qu, Z.-W.; Englert, U.; Bolte, M.; Lerner, H.-W.; Holthausen, M.C.; Wagner, M. Main-chain boron-containing oligophenylenes via ring-opening polymerization of 9-H-9-borafluorene. *J. Am. Chem. Soc.* **2011**, *133*, 4596–4609. [[CrossRef](#)] [[PubMed](#)]
22. Hübner, A.; Diefenbach, M.; Bolte, M.; Lerner, H.-W.; Holthausen, M.C.; Wagner, M. Confirmation of an early postulate: B-C-B two-electron–three-center bonding in organo(hydro)boranes. *Angew. Chem. Int. Ed.* **2012**, *51*, 12514–12518. [[CrossRef](#)] [[PubMed](#)]
23. Kaese, T.; Hübner, A.; Bolte, M.; Lerner, H.-W.; Wagner, M. Forming B–B Bonds by the Controlled Reduction of a Tetraaryldiborane(6). *J. Am. Chem. Soc.* **2016**, *138*, 6224–6233. [[CrossRef](#)]
24. Oliva-Enrich, J.M.; Kondo, T.; Alkorta, I.; Elguero, J.; Klein, D.J. Concatenation of diborane leads to new planar boron chemistry. *Chem. Phys. Chem.* **2020**. [[CrossRef](#)]
25. Rashid, Z.; van Lenthe, J.H. Generation of Kekulé valence structures and the corresponding valence bond wave function. *J. Comput. Chem.* **2010**, *32*, 696–708. [[CrossRef](#)]
26. Cram, D.J.; Tanner, M.E.; Thoams, R. The taming of cyclobutadiene. *Angew. Chem. Int. Ed.* **1991**, *30*, 1024–1027. [[CrossRef](#)]
27. Liu, Y.; Kilby, P.; Frankcombe, T.J.; Schmidt, T.W. The electronic structure of benzene from a tiling of the correlated 126-dimensional wavefunction. *Nature* **2020**, *11*, 1–5. [[CrossRef](#)] [[PubMed](#)]
28. Grimme, S. Semiempirical GGA-type density functional constructed with a long-range dispersion correction. *J. Comp. Chem.* **2006**, *27*, 1787–1799. [[CrossRef](#)] [[PubMed](#)]
29. Ma, J.C.; Dougherty, D.A. The cation–π interaction. *Chem. Rev.* **1997**, *97*, 1303–1324. [[CrossRef](#)] [[PubMed](#)]
30. Alkorta, I.; Rozas, I.; Elguero, J. Interaction of anions with perfluoro aromatic compounds. *J. Am. Chem. Soc.* **2002**, *124*, 8593–8598. [[CrossRef](#)]

31. Geuenich, D.; Hess, K.; Köhler, F.; Herges, R. Anisotropy of the induced current density (ACID), a general method to quantify and visualize electronic delocalization. *Chem. Rev.* **2005**, *105*, 3758–3772. [[CrossRef](#)]
32. Claus, K.H.; Krüger, C. Structure of cyclooctatetraene at 129 K. *Acta Cryst. Sect. C* **1988**, *44*, 1632–1634. [[CrossRef](#)]
33. Krygowski, T.M.; Pindelska, E.; Cyrański, M.K.; Häfelinger, G. Planarization of 1,3,5,7-cyclooctatetraene as a result of a partial rehybridization at carbon atoms: An MP2/6-31G* and B3LYP/6-311G** study. *Chem. Phys. Lett.* **2002**, *359*, 158–162. [[CrossRef](#)]
34. Nishinaga, T.; Ohmae, T.; Iyoda, M. Recent studies on the aromaticity and antiaromaticity of planar cyclooctatetraene. *Symmetry* **2010**, *2*, 76. [[CrossRef](#)]
35. Bally, T.; Chai, S.; Neuenschwander, M.; Zhu, Z. Pentalene: Formation, electronic, and vibrational structure. *J. Am. Chem. Soc.* **1997**, *119*, 1869–1875. [[CrossRef](#)]
36. Hafner, K.; Süß, H.U. 1,3,5-Tri-tert-butylpentalene. A stabilized planar 8π electron system. *Angew. Chem. Int. Ed. Engl.* **1973**, *12*, 575–577. [[CrossRef](#)]
37. Carey, F.A.; Sundberg, R.J. *Advanced Organic Chemistry. Part A: Structure and Mechanisms*, 2nd ed.; Plenum Press: New York, NY, USA, 1984.
38. Mosher, O.A.; Flicker, W.M.; Kuppermann, A. Triplet states in 1,3-butadiene. *Chem. Phys. Lett.* **1973**, *19*, 332–333. [[CrossRef](#)]
39. Gordon, M. The Azulenes. *Chem. Rev.* **1952**, *50*, 127–200. [[CrossRef](#)]
40. Schleyer, P.V.R.; Maerker, C.; Dransfeld, A.; Jiao, H.; Hommes, J.R.V.E. Nucleus-independent chemical shifts: A simple and efficient aromaticity probe. *J. Am. Chem. Soc.* **1996**, *118*, 6317–6318. [[CrossRef](#)] [[PubMed](#)]
41. Becke, A.D. Density-functional thermochemistry. III. The role of exact exchange. *J. Chem. Phys.* **1993**, *98*, 5648–5652. [[CrossRef](#)]
42. Lee, C.; Yang, W.; Parr, R.G. Development of the Colle-Salvetti correlation-energy formula into a functional of the electron density. *Phys. Rev. B* **1988**, *37*, 785–789. [[CrossRef](#)]
43. Vosko, S.H.; Wilk, L.; Nusair, M. Accurate spin-dependent electron liquid correlation energies for local spin density calculations: A critical analysis. *Can. J. Phys.* **1980**, *58*, 1200–1211. [[CrossRef](#)]
44. Stephens, P.J.; Devlin, F.J.; Chabalowski, C.F.; Frisch, M.J. Ab initio calculation of vibrational absorption and circular dichroism spectra using density functional force fields. *J. Phys. Chem.* **1994**, *98*, 11623–11627. [[CrossRef](#)]
45. Frisch, M.J.; Trucks, G.W.; Schlegel, H.B.; Scuseria, G.E.; Robb, M.A.; Cheeseman, J.R.; Scalmani, G.; Barone, V.; Petersson, G.A.; Nakatsuji, H.; et al. *Gaussian 16; Revision C.01*; Gaussian, Inc.: Wallingford, CT, USA, 2016.

Sample Availability: Samples of the compounds are not available from the authors.

Publisher's Note: MDPI stays neutral with regard to jurisdictional claims in published maps and institutional affiliations.



© 2020 by the authors. Licensee MDPI, Basel, Switzerland. This article is an open access article distributed under the terms and conditions of the Creative Commons Attribution (CC BY) license (<http://creativecommons.org/licenses/by/4.0/>).